Electronic Supplementary Information

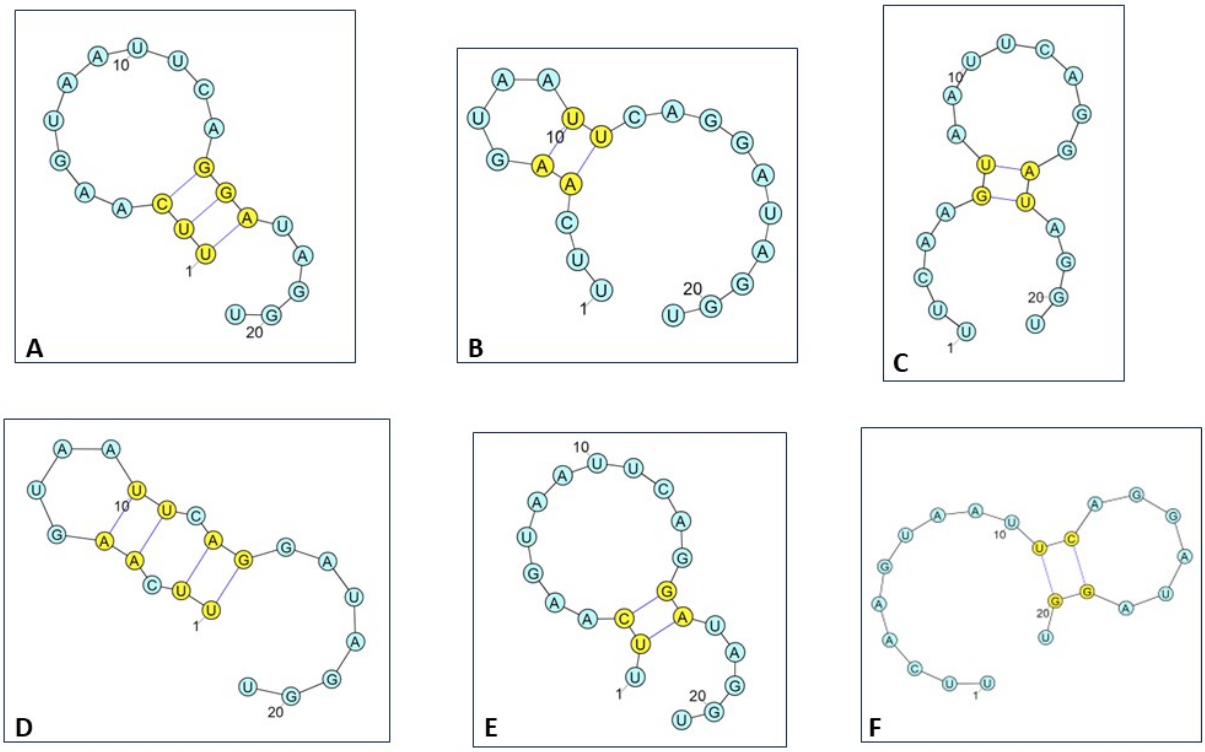

Fig. S1 Cartoon representations of all the possible secondary structures of the miR-26b-5p sequence, as predicted by mFold[1]. 'Structure A' represents the most stable configuration, which is also provided by RNAstructure[2]. Cartoon representations were created using RiboSketch[3].

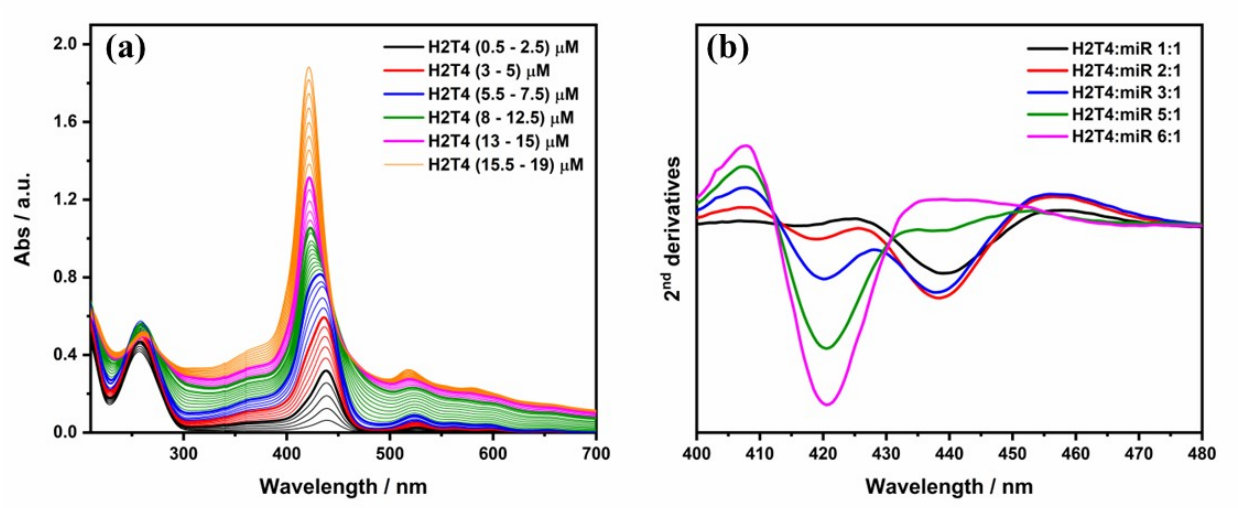

Fig. S2 (a) UV-vis titration of miR-26b-5p [2.5 μM] in PBS buffer in the presence of increasing amount of H2T4 (from 0.5 μM to 19 μM). Each addition of 0.5 μM of H2T4. Bold lines represent the concentration in which there is a change of the molar extinction coefficient. Displayed colors are the same used in the "plot of absorbance at 421 nm vs. the ratio [H2T4]/[miR-26b-5p]" (**Fig.3, inset**). **(b)** 2nd derivatives of UV-vis spectra of H2T4 (at the break points) in the presence of the miRNA.

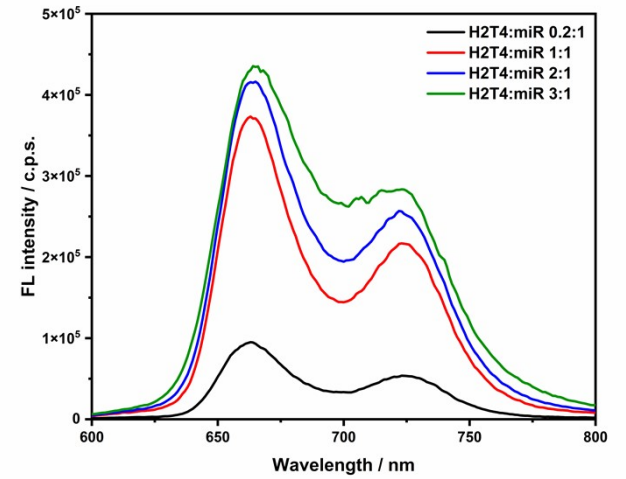

Fig. S3 Fluorescence titration of miR-26b-5p [2.5 µM] in PBS buffer in the presence of increasing amount of H2T4 (0.5 µM black curve; 2.5 µM red curve; 5 µM blue curve; 7.5 µM green curve).

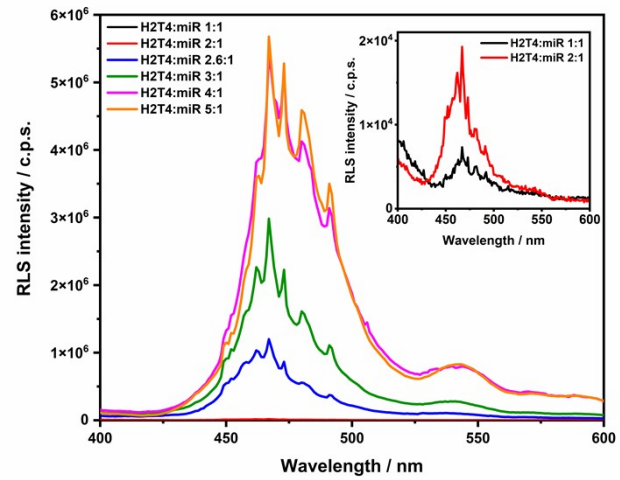

Fig. S4 RLS titration of miR-26b-5p [2.5 µM] in PBS buffer in the presence of increasing amount of H2T4 (2.5 µM black curve; 5 µM red curve; 6.5 µM blue curve; 7.5 µM green curve; 10 µM magenta curve; 12.5 µM orange curve).

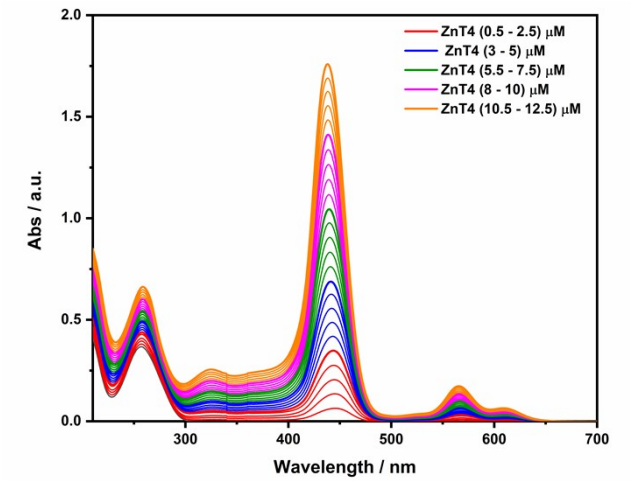

Fig. S5 UV-vis titration of miR-26b-5p [2.5 μM] in PBS buffer in the presence of increasing amount of Zn2T4 (from 0.5 μM to 12.5 μM). Each addition of ZnT4 of 0.5 μM.

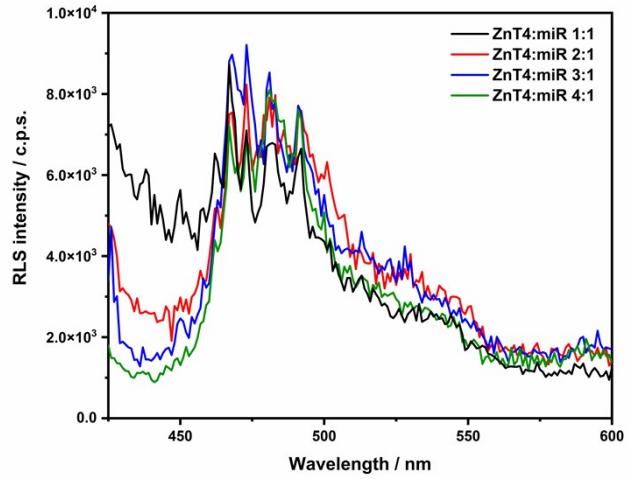

Fig. S6 RLS titration of miR-26b-5p [2.5 μM] in PBS buffer in the presence of increasing amount of ZnT4 (2.5 μM black curve; 5 μM red curve; 7.5 μM blue curve; 10 μM green curve.

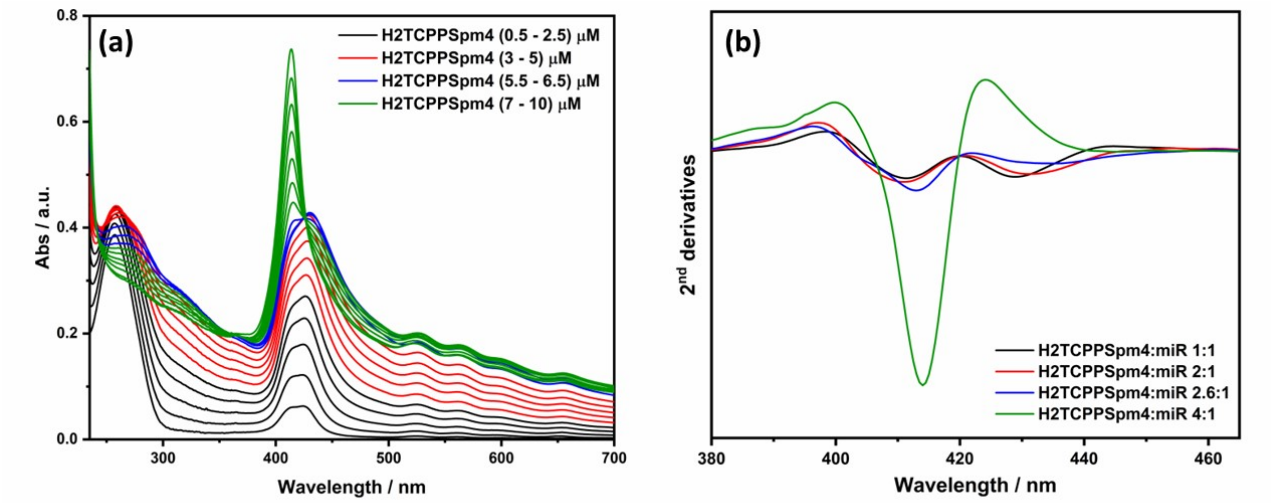

Fig. S7 (a) UV-vis titration of miR-26b-5p [2.5 μM] in PBS buffer in the presence of increasing amount of H2TCPPSpm4 (from 0.5 μM to 10 μM). Each addition of 0.5 μM of H2TCPPspm4. Displayed colors are the same used in the "plot of absorbance at 414 nm vs. the ratio [H2TCPPSpm4] / [miR-26b-5p]" (**Fig.8, inset**). **(b)** 2nd derivatives of UV-vis spectra of H2TCPPSpm4 (at the break points) in the presence of the miRNA.

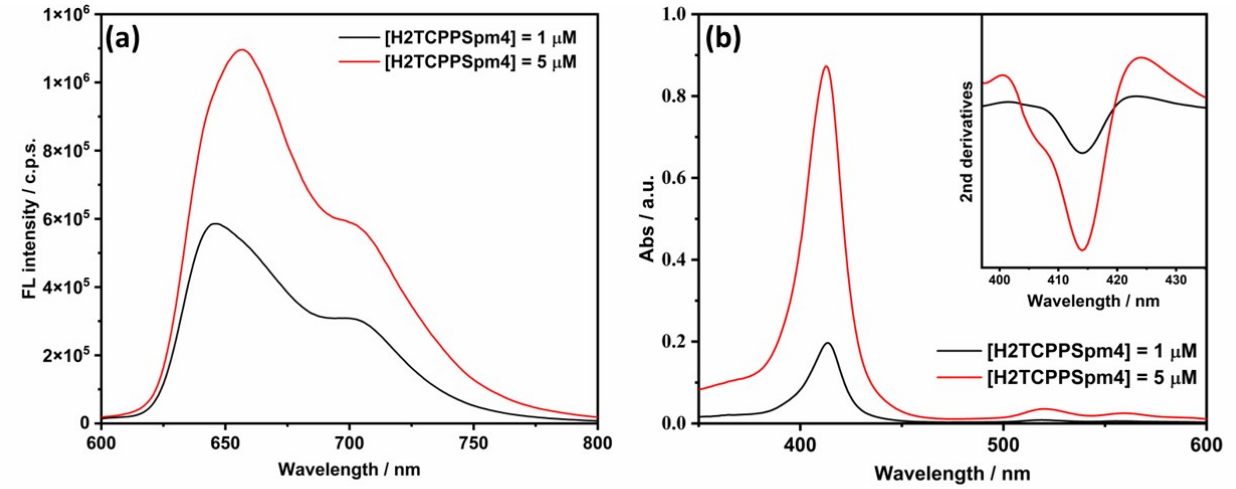

Fig. S8 (a) Emission spectra of H2TCPPSpm4 [1 μM] (black curve) and [5 μM] (red curve) in PBS buffer. **(b)** Absorption spectra of H2TCPPSpm4 [1 μM] (black curve) and [5 μM] (red curve) in PBS buffer. Inset: second derivatives of H2TCPPSpm4 [1 μM] (black curve) and [5 μM] (red curve).

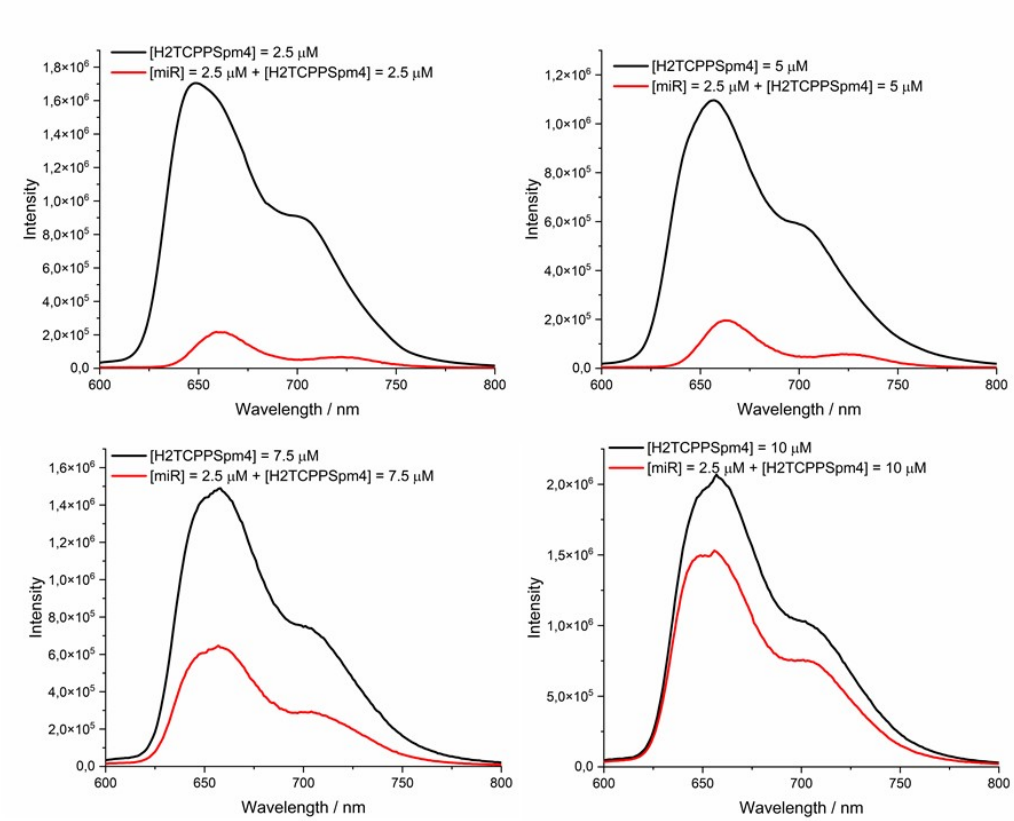

Fig. S9 Emission spectra of H2TCPPSpm4 (black curve) at different concentrations and in the presence of miR-26b-5p [2.5 μM] (red curve) in PBS buffer.

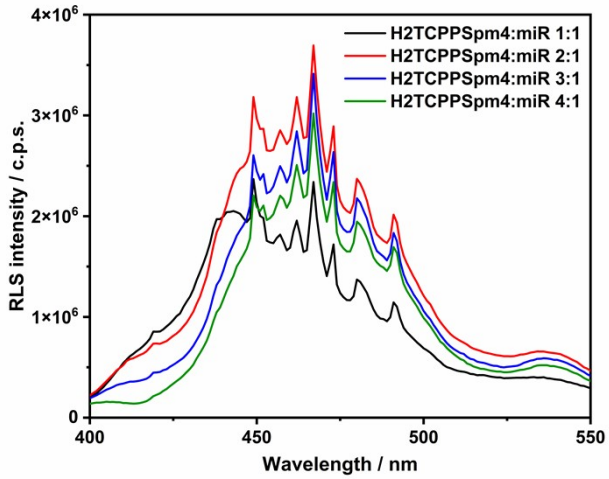

Fig. S10 RLS titration of miR-26b-5p [2.5 μM] in PBS buffer in the presence of increasing amount of H2TCPPSpm4 (2.5 μM black curve; 5 μM red curve; 7.5 μM blue curve; 10 μM green curve).

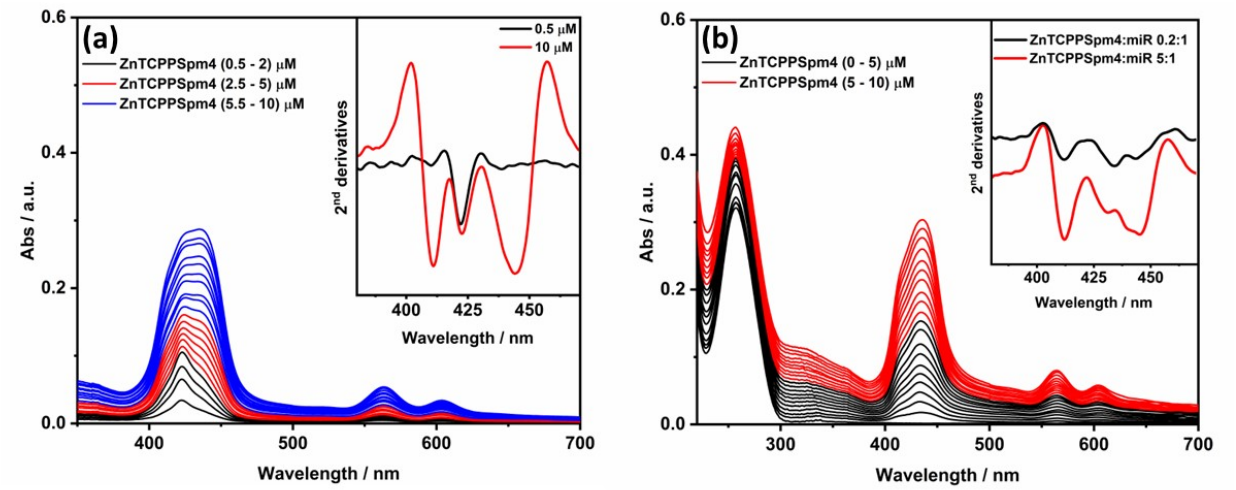

Fig. S11 (a) UV-vis titration of increasing amount of ZnTCPPSpm4 (from 0.5 μM to 10 μM) in PBS buffer. Each addition of 0.5 μM of ZnTCPPspm4. Inset: 2nd derivatives of UV-vis spectra of ZnTCPPSpm4 at the concentration of 0.5 μM (black line) and 10 μM (red line). **(b)** UV-vis titration of miR-26b-5p [2.5 μM] in PBS buffer in the presence of increasing amount of ZnTCPPSpm4 (from 0.5 μM to 10 μM). Each addition of 0.5 μM of ZnTCPPspm4. Inset: 2nd derivatives of UV-vis spectra of ZnTCPPSpm4 at the concentration of 0.5 μM (black line) and 10 μM (red line) in presence of miR.

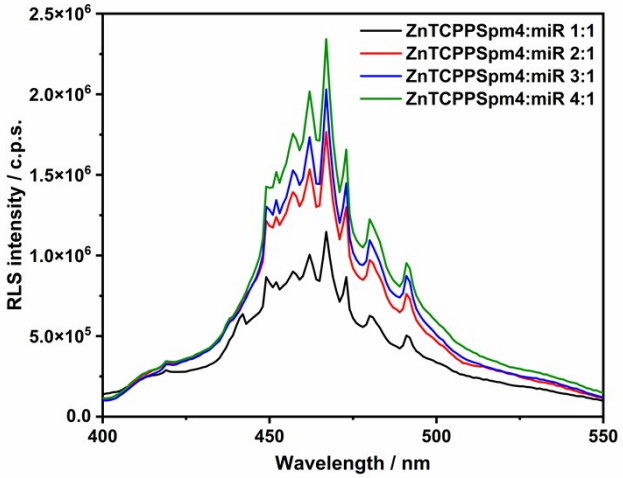

Fig. S12 RLS titration of miR-26b-5p [2.5 μM] in PBS buffer in the presence of increasing amount of ZnTCPPSpm4 (2.5 μM black curve; 5 μM red curve; 7.5 μM blue curve; 10 μM green curve).

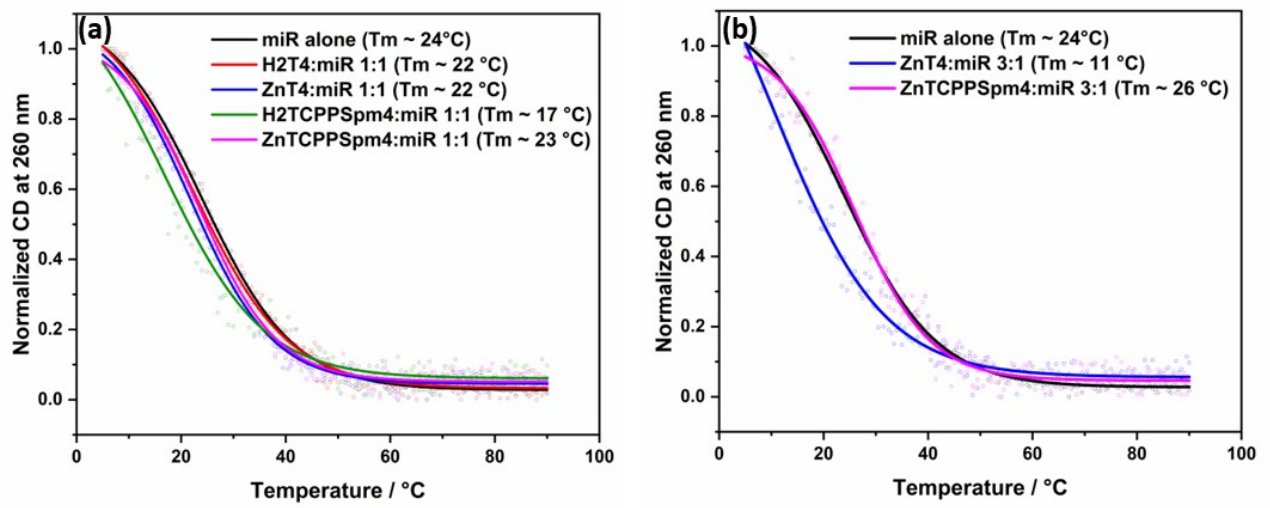

Fig. S13 (a) Normalized CD melting curves of miR-26b-5p [2.5 μM] alone in PBS buffer (black line) and with the presence of H2T4 [2.5 μM] (red line), ZnT4 [2.5 μM] (blue line), H2TCPPSpm4 [2.5 μM] (green line) and ZnTCPPspm4 [2.5 μM] (magenta line), respectively. **(b)** Normalized CD melting curves of miR-26b-5p [2.5 μM] in PBS buffer with the presence of H2T4 [7.5 μM] (red circles), ZnT4 [7.5 μM] (blue line) and ZnTCPPspm4 [7.5 μM] (green line), respectively.

Scatchard plots and apparent association constants

The titration data were treated with Peacocke-Sherrett method's[4] in order to calculate the values of ν (number of moles of bound porphyrin per mole of total miRNA) and L (molar concentration of free porphyrin at equilibrium) needed to graph the Scatchard plot (**Fig. S13**).

At each intermediate titration point, the fraction of bound porphyrin was calculated by the use of the expression $\alpha = (A_f - A)/(A_f - A_b)$, where A_f is the absorption at the Soret maximum for free porphyrin (421 nm for H2T4, 436 nm for ZnT4, 414 nm for H2TCPPSpm4 and 423 nm for ZnTCPPSpm4), A_b is the absorbance at same wavelength of A_f but of a solution in which the miRNA concentration was 25 times greater than the initial concentration of porphyrin (conditions for which complete binding may be assumed) and and A is the absorbance at the Soret maximum of porphyrin at any given point during the titration.

In a typical linear Scatchard plot (**Fig. S13 (a), (c) and (d)**), the slope extrapolation corresponds to K_{app} according to Eq. 1. Thus, our estimated K_{app} values are listed in **Table 1**. Such values align with previously reported data on the interaction between porphyrins and various oligonucleotide structures Specifically, for DNA G-quadruplex structures [5–7] the binding constants typically fall within the range of 10^5 to 10^7. In the case of RNA G-quadruplexes[8] the binding constant is generally around 10^5, while for RNA duplex structures [9,10] it typically ranges from 10^4 to 10^5. For ZnT4 was not possible to obtain the K_{app} because the Scatchard plot significantly deviates from linearity with an upward curvature (**Fig. S13 (b)**). The latter arises as a consequence of cooperativity and neighbor exclusion effects[11] suggesting a negative co-operativity binding of ZnT4 with miR-26b-5p. This negative cooperative binding behavior and curvature in the Scatchard plot could be attributed to very weak binding interactions between the porphyrin and miRNA, consistent with the spectroscopic results. In fact, the weaker the interactions, the more difficult it is for multiple porphyrins to bind to the miRNA, leading to non-linearity in the Scatchard plot. However, excluding the first three points, the fit appears almost linear. Indeed, excluding these first three points, a linear correlation coefficient of 1.57×10^5 with an adjusted R-squared of 0.95 and Pearson's R of -0.97 was obtained. It is the lowest value of K_{app}, in comparison to other K_{app} values, which aligns with our spectroscopic data, which indicates that ZnT4 porphyrin interacts weakly with the miRNA.

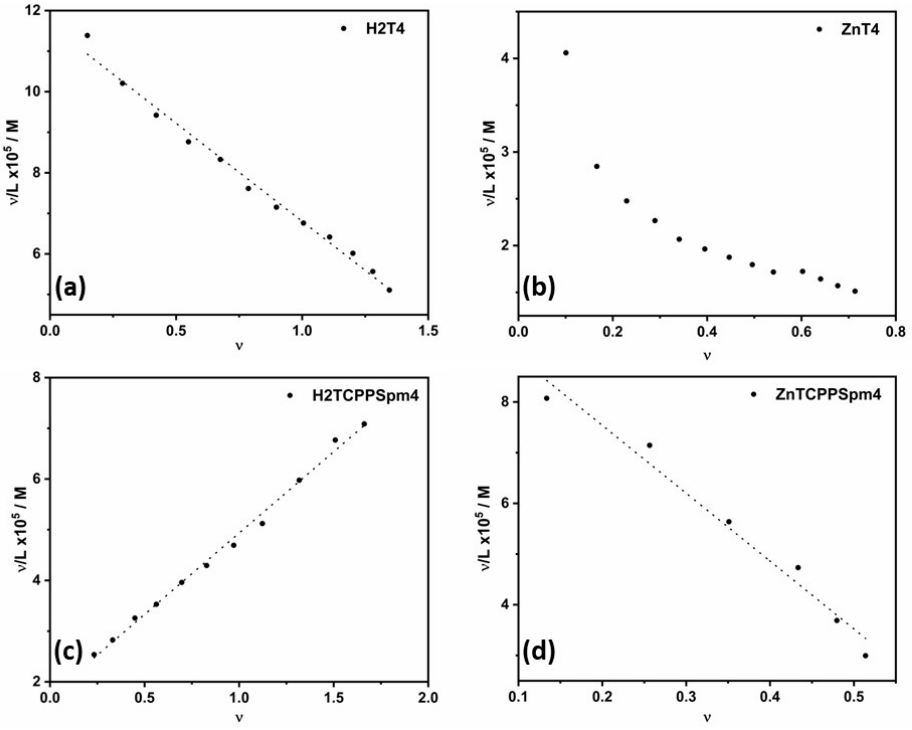

Fig. S14 Scatchard plots for titration of miR-26b-5p with H2T4 **(a),** ZnT4 **(b),** H2TCPPSpm4 **(c)** and ZnTCPPSpm4 **(d).**

References

1 M. Zuker, *Nucleic Acids Res*, 2003, **31**, 3406–3415.

2 S. Bellaousov, J. S. Reuter, M. G. Seetin and D. H. Mathews, *Nucleic Acids Res*, 2013, **41**, W471–W474.

3 J. S. Lu, E. Bindewald, W. K. Kasprzak and B. A. Shapiro, *Bioinformatics*, 2018, **34**, 4297–4299.

4 A. R. Peacocke and J. N. H. Skerrett, *Transactions of the Faraday Society*, 1956, **52**, 261–279.

5 L. R. Keating and V. A. Szalai, *Biochemistry*, 2004, **43**, 15891–15900.

6 L. Guo, W. Dong, X. Tong, C. Dong and S. Shuang, *Talanta*, 2006, **70**, 630–636.

7 N. C. Sabharwal, J. Chen, J. H. J. Lee, C. M. A. Gangemi, A. D'urso and L. A. Yatsunyk, *Int J Mol Sci*, 2018, **19**, 3686.

8 Q. Qi, C. Yang, Y. Xia, S. Guo, D. Song and H. Su, *Journal of Physical Chemistry Letters*, 2019, **10**, 2143–2150.

9 A. A. Ghazaryan, Y. B. Dalyan, S. G. Haroutiunian, A. Tikhomirova, N. Taulier, J. W. Wells and T. V. Chalikian, *J Am Chem Soc*, 2006, **128**, 1914–1921.

10 T. Uno, K. Hamasaki, M. Tanigawa and S. Shimabayashi, *Inorg Chem*, 1997, **36**, 1676–1683.

11 J. D. McGhee and P. H. von Hippel, *J Mol Biol*, 1974, **86**, 469–489.